

Accepted Manuscript

Synthesis and evaluation of nicotinamide derivative as anti-angiogenic agents

Hye-Eun Choi, Jung-Hye Choi, Jae Yeol Lee, Je Hak Kim, Ji Han Kim, Joon Kwang Lee, Gyu Il Kim, Yong Park, Yong Ha Chi, Soo Heui Paik, Joo Han Lee, Kyung-Tae Lee

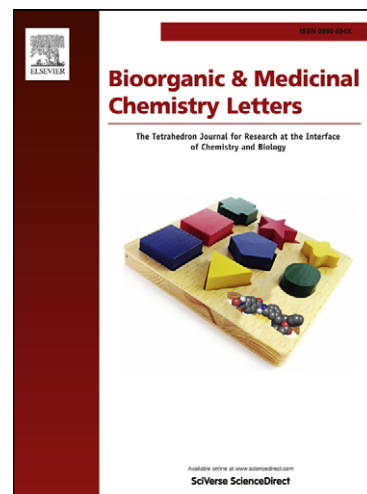
PII: S0960-894X(13)00158-3
DOI: <http://dx.doi.org/10.1016/j.bmcl.2013.01.125>
Reference: BMCL 20113

To appear in: *Bioorganic & Medicinal Chemistry Letters*

Received Date: 1 November 2012
Revised Date: 14 January 2013
Accepted Date: 30 January 2013

Please cite this article as: Choi, H-E., Choi, J-H., Lee, J.Y., Kim, J.H., Kim, J.H., Lee, J.K., Kim, G.I., Park, Y., Chi, Y.H., Paik, S.H., Lee, J.H., Lee, K-T., Synthesis and evaluation of nicotinamide derivative as anti-angiogenic agents, *Bioorganic & Medicinal Chemistry Letters* (2013), doi: <http://dx.doi.org/10.1016/j.bmcl.2013.01.125>

This is a PDF file of an unedited manuscript that has been accepted for publication. As a service to our customers we are providing this early version of the manuscript. The manuscript will undergo copyediting, typesetting, and review of the resulting proof before it is published in its final form. Please note that during the production process errors may be discovered which could affect the content, and all legal disclaimers that apply to the journal pertain.



[Bioorganic & Medicinal Chemistry Letters]

Synthesis and evaluation of nicotinamide derivative as anti-angiogenic agents

Hye-Eun Choi^{a,b}, Jung-Hye Choi^{b,c}, Jae Yeol Lee^d, Je Hak Kim^e, Ji Han Kim^e, Joon Kwang Lee^f, Gyu Il Kim^e, Yong Park^e, Yong Ha Chi^e, Soo Heui Paik^e, Joo Han Lee^e and Kyung-Tae Lee^{a,b*}

^a*Department of Pharmaceutical Biochemistry,* ^b*Department of Life and Nanopharmaceutical Science, and* ^c*Department of Oriental Pharmaceutical Science, College of Pharmacy, Kyung Hee University, 1 Hoegi-dong, Dongdaemun-gu, Seoul 130-701, Republic of Korea*

^d*Research Institute for Basic Sciences and Department of Chemistry, College of Sciences, Kyung Hee University, Seoul 130-701, Republic of Korea*

^e*Central Research Institute, Boryung Pharm. Co. Ltd., 1122-3, Shingil-Dong, Danwon-Gu, Ansan-Si, Kyungki-Do, 425-839, Republic of Korea*

* Corresponding author.

Tel; +82-2-9610860; fax: +82-2-9620860

E-mail address: ktleee@khu.ac.kr(K-T Lee).

ABSTRACT

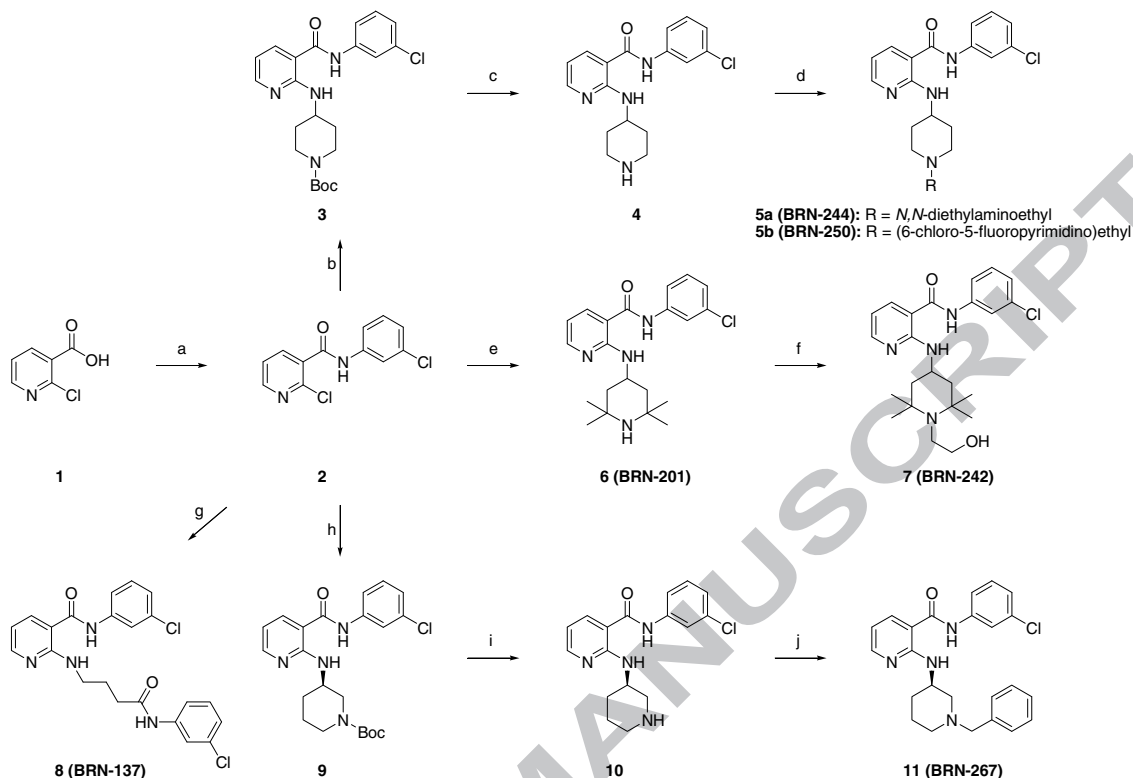
Previously, we have found that **BRN-103**, a nicotinamide derivative, inhibits vascular endothelial growth factor (VEGF)-mediated angiogenesis signaling in human endothelial cells. During our continuous efforts to identify more potent anti-angiogenic agents, we synthesized various nicotinamide derivatives and evaluated their anti-angiogenic effects. We found that 2-{1-[1-(6-chloro-5-fluoropyrimidin-4-yl)ethyl]piperidin-4-ylamino}-*N*-(3-chlorophenyl) pyridine-3-carboxamide (**BRN-250**) significantly inhibited human umbilical vascular endothelial cells (HUVECs) proliferation, migration, tube formation, and microvessel growth in a concentration range of 10-100 nM. Furthermore, **BRN-250** inhibited the VEGF-induced phosphorylation and intracellular tyrosine kinase activity of VEGF receptor 2 (VEGFR2) and the activation of its downstream AKT pathway. Taken together, these findings suggest that **BRN-250** be considered a potential lead compound for cancer therapy.

Keywords: Anti-angiogenesis, Nicotinamide, VEGFR, HUVECs, Receptor tyrosine kinase

Angiogenesis is the process of the formation of new blood vessels from preexisting blood vessels, and includes the destabilization of established vessels, endothelial cell proliferation and migration, and the degradation of extra-cellular matrix, and the formation and sprouting of new vessels.^{1,2,3} On the other hand, tumor angiogenesis is the process whereby the network of blood vessels expands and penetrates cancerous growths to supply nutrients and oxygen and remove metabolic waste from tumors. The inhibition of angiogenesis is referred to as the fourth modality of anticancer therapy.⁴

Vascular endothelial growth factor (VEGF) is a crucial regulator of angiogenesis,^{5,6} and acts on endothelial cells as a chemotactic and mitogenic factor via endothelial cell-specific receptors, that is vascular endothelial growth factor receptor1 (VEGFR1) (Flt-1), VEGFR2 (Flk-1/KDR) and VEGFR3 (Flt-4), of which VEGFR2 is the major mediator of the pro-angiogenic effects induced by VEGF.⁷ In addition, tumor cells release several pro-angiogenic factors that enhance metastasis, and therefore, shorten patient survival.⁸ Although antibodies against VEGF (avastin) or multi-targeting inhibitors of receptor tyrosine kinase (RTK) (sorafenib and sunitinib) have already been approved by the US Food and Drug Administration (FDA) for advanced renal cancer, safer and more efficient inhibitors are still needed.^{9,10} The anti-angiogenic and direct anti-tumor effects of sunitinib may be important aspects of its anti-tumor activity, at least for certain tumor types.¹¹

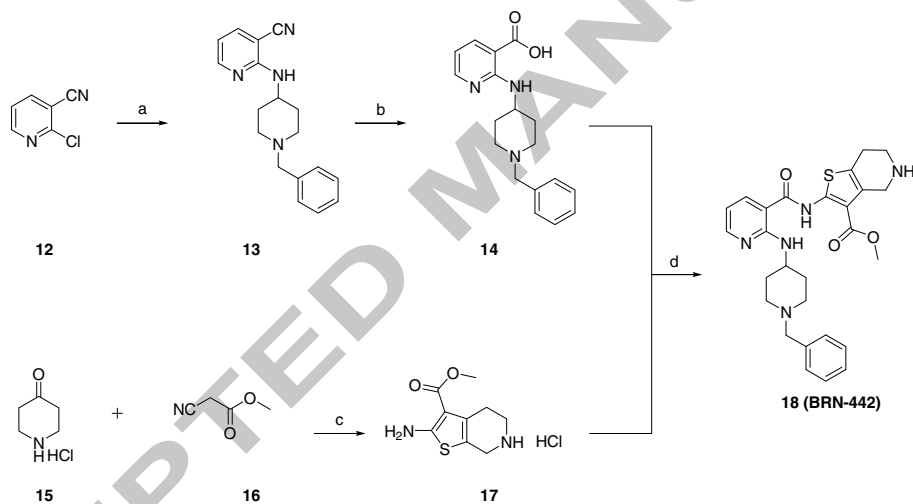
In the present study, we have constructed the library of nicotinamide derivatives using the general reaction pathway outlined in Scheme 1-2 based on the previously biological activity of **BRN-103** (a nicotinamide derivative) against angiogenesis¹² and examined the abilities of these compounds to inhibit VEGF-induced HUVEC proliferation at concentrations less than their IC₉₀ values (data not shown) using 5-bromo-2-deoxyuridine (BrdU) incorporation method.¹³



Scheme 1. Reagents and conditions: (a) i) SOCl_2 , DCM, reflux, 1.5 h; ii) 3-chloroaniline, Et_3N , 12 h, 82%; (b) 4-amino-1-Boc-piperidine, K_2CO_3 , xylene, 130 °C, 24 h, 42%; (c) *conc.* HCl, EtOH, reflux, 4 h, 90%; (d) *N,N*-diethylaminoethyl chloride or 4-(1-bromoethyl)-6-chloro-5-fluoropyrimidine, K_2CO_3 , ACN, reflux, 24 h, 45% for **5a** and 48% for **5b**; (e) 4-amino-2,2,6,6-tetramethylpiperidine, K_2CO_3 , xylene, 130 °C, 24 h, 82%; (f) 2-bromoethanol, K_2CO_3 , ACN, reflux, 18 h, 37%; (g) *N*-(3-chlorophenyl)-4-aminobutanamide, K_2CO_3 , xylene, 130 °C, 24 h, 83%; (h) (*R*)-3-amino-1-Boc-piperidine, K_2CO_3 , xylene, 130 °C, 24 h, 44%; (i) *conc.* HCl, EtOH, reflux, 4 h, 64%; (j) benzyl chloride, K_2CO_3 , ACN, reflux, 18 h, 68%.

The synthetic methods used to construct the nicotinamide library began with the 2-chloronicotinic acid (**1**) and 2-chloro-3-cyanopyridine (**12**), respectively (Scheme 1 and 2). 2-Chloronicotinic acid could be carried forward directly for the 2-chloronicotinamide derivative (**2**), which was substituted with various amines to afford the corresponding 2-aminonicotinamide derivatives [**3**, **6 (BRN-201)**, **8 (BRN-137)** and **9**]. In the case of compound **3** and **9**, the de-protection of Boc group and subsequent *N*-alkylation with *N,N*-diethylaminoethyl chloride, 4-(1-bromoethyl)-6-chloro-5-fluoropyrimidine¹⁴ and benzyl

chloride to give the compound **5a** (BNR-244), **5b** (BRN-250)¹⁵ and **11** (BRN-267), respectively. Compound **6** (BRN-201) containing 2,2,6,6-tetramethylpiperidine ring was directly *N*-alkylated with 2-bromoethanol to provide compound **7** (BRN-242). In the case of compound **18** (BRN-442) containing 4,5,6,7-tetrahydrothieno[2,3-*c*]pyridine-3-carboxylate, this fused heterocycle (**17**) was easily prepared from the reaction of 4-piperidone (**15**) with methyl cyanoacetate (**16**) in the presence of sulfur¹⁶ and could be acylated with 2-aminonicotinic acid (**14**) using thionyl chloride resulted in the compounds **18** as shown in Scheme 2.



Scheme 2. Reagents and conditions: (a) 4-amino-1-benzylpiperidine, K_2CO_3 , xylene, 140 °C, 40 h, 72% ; (b) KOH, IPA, reflux, 20 h, 88%; (c) sulfur, Et_2NH , MeOH, 5 h, 43% (d) i) $SOCl_2$, DCM, reflux, 1 h; ii) compound **17**, Et_3N , reflux, 4 h, 83%.

It was found that some of these compounds displayed potent inhibitory effects, and that 2-{1-[1-(6-chloro-5-fluoropyrimidin-4-yl)ethyl]piperidin-4-ylamino}-*N*-(3-chlorophenyl)pyridine-3-carboxamide (BRN-250) most effectively inhibited VEGF-induced HUVEC proliferation (Figure 1A). In addition, BRN-250 was found to inhibit VEGF-induced HUVEC proliferation concentration-dependently and to be more potent in this respect than

BRN-103 (Figure 1B).

To further assess the anti-angiogenic property of **BRN-250** *in vitro*, we examined its inhibitory effects on the migration of endothelial cells using the wound-healing and the Trans-well assays. As shown in Figure 2A, **BRN-250** (10, 50, or 100 nM) significantly inhibited VEGF-induced HUVEC migration in the wound-healing assay. In the Trans-well assay – the most popular *in vitro* test of angiogenesis,¹⁷ cells were seeded onto the upper surface of an 8 μ m pore size membrane separating upper and lower Boyden's chambers. The upper chamber contained **BRN-250** in 0.1% endothelial basal medium (EBM), and cellular migration through the membrane was induced when VEGF was introduced in the lower chamber. Using this assay, we found that **BRN-250** dramatically reduced cell migration (Figure 2B). **BRN-250** was found to inhibit endothelial migration dose-dependently by both assays and to have a significant inhibitory effect at 10 nM.

Although several types of cells participate in angiogenesis, tube formation by endothelial cells is a key step.¹⁸ Therefore, we investigated whether **BRN-250** regulates capillary tube formation by HUVECs.¹⁹ When HUVECs were seeded on growth factor reduced two-dimensional Matrigel, robust tubular structures were formed in the presence of VEGF (10 ng/ml). However, preincubation with **BRN-250** (10, 50, or 100 nM) markedly and dose-dependently abolished this tube formation (Figure 3A). To determine whether **BRN-250** influences VEGF-induced angiogenesis *ex vivo*, the sprouting of vessels from rat aortic rings²⁰ were examined in the presence or absence of **BRN-250** (10, 50, or 100 nM). As shown in Figure 3B, VEGF significantly stimulated microvessel sprouting, which led to the formation of a network of vessels around rat aortic rings. On the other hand, **BRN-250** dose-dependently antagonized VEGF-induced sprouting.

VEGF family members are best known as a family of potent angiogenesis factors,

and are believed to act as angiogenesis switches to trigger the expansion of quiescent tumor tissues.^{21,22} Furthermore, the VEGF-related pathway has become an attractive target because some VEGF inhibitors have already been shown to possess potent anti-tumor effects *in vivo* and *in vitro*.²³ VEGFRs and their signaling pathways represent rate-limiting steps in physiologic angiogenesis.^{24,25} In particular, VEGFR2 is the primary mediator of the angiogenic activity of VEGF via distinct signal transduction pathways that regulate endothelial cell proliferation, migration, differentiation, and tube formation. The major autophosphorylation site on VEGFR2 has been reported to be located at Tyr¹¹⁷⁵, and its phosphorylation provides a docking site with the p85 subunit of PI3K and with phosphoinositidephospholipase C γ (PLC γ).^{26,27,28} Furthermore, this phosphorylation is critical for subsequent VEGF-stimulated proliferation, chemotaxis and sprouting, and for the survival of cultured endothelial cells *in vitro* and *in vivo*.²⁶

Since growth factor-induced endothelial cell migration and subsequent tube formation are known to be PI3K-AKT-dependent,^{29,30} activation of the AKT pathway has been established to play a crucial role in malignant transformation, chemoresistance, and invasiveness by inducing cell survival, growth, migration, and angiogenesis.³¹ Therefore, to elucidate the molecular mechanism that underlies the anti-angiogenic effect of **BRN-250**, we examined its effect on the activation of VEGFR2 and on AKT downstream of VEGFR2. As shown in Figure 4A, **BRN-250** significantly and dose-dependently suppressed the VEGF-induced phosphorylations of VEGFR2 (Tyr¹¹⁷⁵) and AKT (Ser⁴⁷³) in HUVECs. Furthermore, **BRN-250** pretreatment dose-dependently suppressed the VEGF-induced intracellular tyrosine kinase activity of VEGFR2 (Tyr¹¹⁷⁵) (Figure 4B). Sunitinib is a multi-targeting inhibitor of receptor tyrosine kinases (RTKs) and has been shown to be effective treatment for several human cancers.²⁶ We found that **BRN-250** was more potently inhibited the VEGF-induced

tyrosine kinase activity of VEGFR (Tyr¹¹⁷⁵) than sunitinib or **BRN-103**. Accordingly, these results suggest that **BRN-250** inhibits angiogenesis by blocking the VEGFR and AKT signaling pathways.

In order to gain more insight of the binding modes of BRN series with a receptor of known X-ray structure, docking studies were carried out using Molegro Virtual Docker (MVD) 2010.4.2 for Windows.³² The reported crystal structure of VEGFR2 with benzimidazole-urea derivative from Protein Data Bank (PDB ID 2OH4) with resolution 2.05 Å was downloaded for the present docking study.³³ The active site of the receptor was defined to include residues within a 10.0 Å radius of benzimidazole-urea atoms. The docking wizard of MVD 2010.4.2 was used to dock the selected **BRN-137**, **-242**, **-250**, or benzimidazole-urea (for docking comparison) on the active sites of VEGFR2. The most stable docking pose was selected by Mol Dock Score predicted by the MVD scoring function for each compound (Table 1). The most active compound **BRN-250** was found to dock into the active site of VEGFR2 with a higher Mol Dock Score and interaction energy than **BRN-137** or **BRN-242**, which was consistent with real experimental results (Table 1).

On finishing point of docking process, the resulting conformation poses of **BRN-250** in the binding sites of VEGFR2 were considered. The detailed binding pattern of **BRN-250** is shown in Figures 5A and 5B. As shown in Figure 5A, the most binding interacted pose of **BRN-250** is shown to be docked into the active site of VEGFR2 and also its binding mode is very similar to that of benzimidazole-urea (the control ligand), which has the extra-binding interaction with the receptor using the 2-carbamate group of benzimidazole ring resulting in the higher MolDock Score and interaction energy. On the other hand, **BRN-250** in Figure 5B showed four hydrogen bond interactions with Glu⁸⁸³ (amide NH of nicotinamide ring), Cys⁹¹⁷ (N atom of pyrimidine ring), and Asp¹⁰⁴⁴ (amide NH of nicotinamide ring & 2-amino

group of pyridine ring), which were similar to the three hydrogen bond interactions of benzimidazole-urea at Cys⁹¹⁷ and Asp¹⁰⁴⁴ in x-ray crystal structure (PDB ID 2OH4).

In summary, nicotinamide derivatives were synthesized and evaluated with respect to their inhibitory activities on VEGF-induced HUVEC cell proliferation. **BRN-250** was found to have greatest inhibitory activity. In addition, **BRN-250** inhibited VEGF-induced HUVEC migration, tube formation, and microvessel sprouting by interfering with the activation of VEGFR2 and its AKT signaling. These results suggest that **BRN-250** should be considered a potential lead compound for the development of novel anti-angiogenic drugs.

Figure 1. BRN-250 inhibited the VEGF-induced proliferation of HUVECs. HUVECs were pre-treated with (A) six BRN compounds (BRN-137, -201, -242, -250, -267, or -442) at a concentration of 100 nM and (B) various concentrations (10, 50, or 100 nM) of BRN-250 1h prior to 24 h of VEGF treatment (10 ng/ml). VEGF-induced cell proliferation was quantified using BrdU incorporation assays. Columns represent the means of three different experiments, and bars represent SD. # $p < 0.05$ vs. non-treated control group, ** $p < 0.01$, *** $p < 0.001$ vs. VEGF-stimulated group; statistical significances were compared using ANOVA and Dunnett's post-hoc test.

Figure 2. BRN-250 inhibited the VEGF-induced migration of HUVECs. (A) Representative photomicrographs of wound healing assays. Using near confluent HUVECs in 60mm culture dish and a scraper, wound was produced. HUVECs were pretreated with BRN-250 (10, 50 or 10 nM) for 1 h before the induction of cellular migration with VEGF (10 ng/ml). After 24 h of incubation, picture was taken. Dotted lines show the area occupied by the initial scraping. (B) HUVECs were cultured in a Boyden chamber, with VEGF (10 ng/ml) in the lower chamber and various concentrations of BRN-250 in the upper chamber. After 24 h, cellular migration was determined by counting cells migrated through the pores. The bar graphs show average numbers of HUVECs that migrated through the membrane. Columns represent the means of three different experiments, and bars represent SD. # $p < 0.05$ vs. non-treated control group, ** $p < 0.01$, *** $p < 0.001$ vs. VEGF-stimulated group; statistical significances were compared using ANOVA and Dunnett's post-hoc test.

Figure 3. BRN-250 inhibited VEGF-induced capillary structure formation and microvessel sprouting *ex vivo*. (A) After being incubated with BRN-250, HUVECs were fixed, and

tubular structures were photographed (magnification, $\times 100$). Tube-like structures were quantified by manual counting in low power fields. Columns represent the means of three different experiments, and bars represent SD. $^{\#}p < 0.05$ vs. non-treated control group, $^{***}p < 0.001$ vs. VEGF-stimulated group; statistical significances were compared using ANOVA and Dunnett's post-hoc test. (B) Aortic segments isolated from SD Rat were placed in Matrigel-covered wells and treated with VEGF in the presence or absence of **BRN-250** (10, 50, or 100 nM). The results shown are representative of three independent experiments, and the photographs of microvessel sprouting from the margins of aortic rings are also representative of three separate experiments.

Figure 4. **BRN-250** inhibited the VEGF-induced activations of VEGFR2 and AKT signaling in HUVECs. (A) HUVECs were stimulated with VEGF (10 ng/ml) for the indicated time periods with or without 1 h of **BRN-250** (10, 50 or 100 nM) pretreatment. Phosphorylation of VEGFR (5min) and Akt (30 min) were examined using Western blot analysis. (B) HUVECs were pretreated with different concentrations of **BRN-250** (10, 50 or 100 nM) 1 h prior to being treated for 5 min with VEGF (10 ng/ml). Phosphorylation of VEGFR2 at Tyr¹¹⁷⁵ was detected by PathScan ELISA kit. The results represent the means of three different experiments, and bars represent SD. $^{\#}p < 0.05$ vs. non-treated control group, $^{***}p < 0.001$ vs. VEGF-stimulated group; statistical significances were compared using ANOVA and Dunnett's post-hoc test.

Figure 5. The pose adopted by **BRN-250** (green carbon) and the control ligand (red carbon) in the active site of VEGF receptor 2 (PDB ID 2OH4). The figure was prepared using Ligand Scout. (A) Three-dimensional model of the interaction of **BRN-250** with the VEGFR2

binding site. Interacting amino acids and **BRN-250** are depicted by green and red sticks, respectively. (B) Hydrogen bond interactions are represented by white-dotted lines. The figure was prepared using Molegro Virtual Docker (PDB ID 2OH4).

Acknowledgments

This research was supported by Basic Research Program through the National Research Foundation of Korea (NRF) funded by the Ministry of Education, Science and Technology (2009-0088135).

ACCEPTED MANUSCRIPT

References and notes

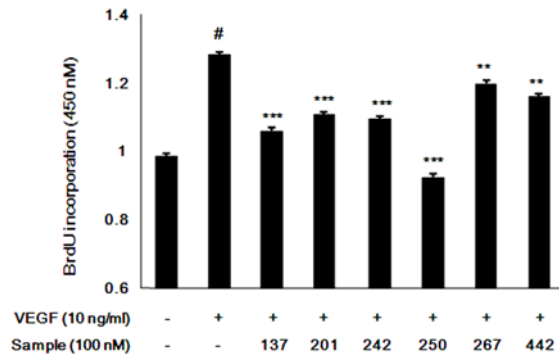
1. Reinhart-King, C. A. *Methods Enzymol.* **2008**, *443*, 45.
2. Tonini, T.; Rossi, F.; Claudio, P. P. *Oncogene* **2003**, *22*, 6549.
3. Folkman, J. *Nat. Med.* **1995**, *1*, 27.
4. Folkman, J. *APMIS.* **2004**, *112*, 496.
5. Yi, Z. F.; Cho, S. G.; Zhao, H.; Wu, Y. Y.; Luo, J.; Li, D.; Yi, T.; Xu, X.; Wu, Z.; Liu, M. *Int. J. Cancer* **2009**, *124*, 843.
6. Yi, T.; Cho, S. G.; Yi, Z.; Pang, X.; Rodriguez, M.; Wang, Y.; Sethi, G.; Aggarwal, B. B.; Liu, M. *Mol. Cancer. Ther.* **2008**, *7*, 1789.
7. Tang, N.; Wang, L.; Esko, J.; Giordano, F. J.; Huang, Y.; Gerber, H. P.; Ferrara, N.; Johnson, R. S. *Cancer Cell* **2004**, *6*, 485.
8. Owen, J. L.; Iragavarapu-Charyulu, V.; Gunja-Smith, Z.; Herbert, L. M.; Grosso, J. F.; Lopez, D. M. *J. Immunol.* **2003**, *171*, 4340.
9. Guccione, A. A. *Phys. Ther.* **1991**, *71*, 499.
10. Ocana, A.; Serrano, R.; Calero, R.; Pandiella, A. *Curr. Drug. Targets* **2009**, *10*, 575.
11. Christensen, J. G. *Ann. Oncol.* **2007**, *18 Suppl 10*.
12. Choi, H. E.; Yoo, M.S.; Choi, J. H.; Lee, J. Y.; Kim, J. H.; Kim, J. H.; Lee, J. K.; Kim, G. I.; Park, Y.; Chi, Y. H.; Paik, S. H.; Lee, J. H.; Lee, K. T. *Bioorg. Med. Chem. Lett.* **2011**, *21*, 6236.
13. Lim, H. J.; Lee, S.; Park, J. H.; Lee, K. S.; Choi, H. E.; Chung, K. S.; Lee, H. H.; Park, H. Y. *Atherosclerosis* **2009**, *202*, 446: Cellular proliferation was determined by BrdU incorporation assay using a commercial ELISA kit according to the manufacturer's instructions (Roche, Basel, Switzerland). Briefly, **BRN-250** and VEGF treated cells were incubated with BrdU specific monoclonal antibody. After addition of peroxidase conjugated secondary antibody, substrate and stop solution were added. The amount of BrdU incorporated was determined by measuring the absorbance at 450 nm.
14. Butters, M.; Ebbs, J.; Green, S. P.; MacRae, J.; Morland, M. C.; Murtiashaw, C. W.; Pettman, A. J. *Org. Process Res.* **2001**, *5*, 28.
15. The spectral data of **BRN-250**: mp 156-172 °C; ¹H NMR (400 MHz, CD₃OD) δ 10.58 (1H, s), 8.18 (1H, m, -CO-NH-CH₂-), 8.64 (1H, d, *J* = 7.3 Hz), 8.51 (1H, s),

- 8.16 (1H, dd, $J = 6.4$ and 1.6 Hz), 7.87 (1H, m), 7.58 (1H, m, $J = 8.4$ Hz), 7.38 (1H, d, $J = 8.0$ Hz), 7.22 (1H, s, dd, $J = 8.0$ and 0.8 Hz), 7.11 (1H, dd, $J = 7.6$ and 6.4 Hz), 5.59 (1H, q, $J = 6.8$ Hz), 4.73-4.69 (2H, m), 4.23 (1H, m), 3.62-3.55 (2H, m), 2.30 (2H, m), 1.93-1.85 (5H, m); ^{13}C NMR (100 MHz, CD_3OD) δ 164.19, 152.41, 152.36, 150.99, 149.96, 149.89, 143.37, 138.94, 138.90, 134.04, 129.83, 124.72, 120.85, 119.07, 116.24, 111.50, 48.32, 45.32, 45.24, 30.61, 21.46; HRMS (EI+) Calcd for $\text{C}_{23}\text{H}_{23}\text{Cl}_2\text{FN}_6\text{O}$ 488.1294, found 488.1279.
16. Schultz, M.; Schiemann, K.; Staehle, W. *PCTInt. Appl.* 2,010,112,124, **2010**.
 17. Redmond, E. M.; Cahill, P. A.; Hirsch, M.; Wang, Y. N.; Sitzmann, J. V.; Okada, S. *S. Thromb. Haemost.* **1999**, *81*, 293.
 18. Patan, S. *Cancer Treat. Res.* **2004**, *117*, 3.
 19. Pang, X.; Yi, Z.; Zhang, X.; Sung, B.; Qu, W.; Lian, X.; Aggarwal, B. B.; Liu, M. *Cancer Res.* **2009**, *69*, 5893. HUVECs were pretreated with indicated concentrations of **BRN-250** for 1 h and then seeded onto the Matrigel layer in 24-well plates at a density of 4 to 7×10^4 cells. EBM was with or without 10 ng/ml VEGF. After incubation for 6 h, tubular structure of endothelial cells was photographed using an inverted microscope (Olympus; magnification, $\times 100$).
 20. Pyun, B. J.; Choi, S.; Lee, Y.; Kim, T. W.; Min, J. K.; Kim, Y.; Kim, B. D.; Kim, J. H.; Kim, T. Y.; Kim, Y. M.; Kwon, Y. G. *Cancer Res.* **2008**, *68*, 227. Rat aortas isolated from Sprague-Dawley rats (NIH) were cleaned of periadventitial fat and cut into rings at 1 to 1.5 mm in circumference. The aortic rings were randomized into Matrigel-coated wells and sealed with a 100 μl overlay of Matrigel. VEGF, with or without indicated concentrations of **BRN-250** was added to the wells. As a control, medium alone was assayed. After 7 day, we fixed the microvessels sprouting and photographed it using an Olympus inverted microscope (Olympus; magnification, $\times 100$).
 21. Aniukhovskii, E. P.; Iasinovskaia, F. P. *Biull. Eksp. Biol. Med.* **1977**, *83*, 519.
 22. Longo, R.; Gasparini, G. *Cancer Chemother. Pharmacol.* **2007**, *60*, 151.
 23. Liu, Z.; Yuan, Q.; Zhang, X.; Xiong, C.; Xue, P.; Ruan, J. *Cancer Chemother. Pharmacol.* **2012**, *69*, 1633.
 24. Brunelleschi, S.; Penengo, L.; Santoro, M. M.; Gaudino, G. *Curr. Pharm. Des.* **2002**, *8*, 1959.

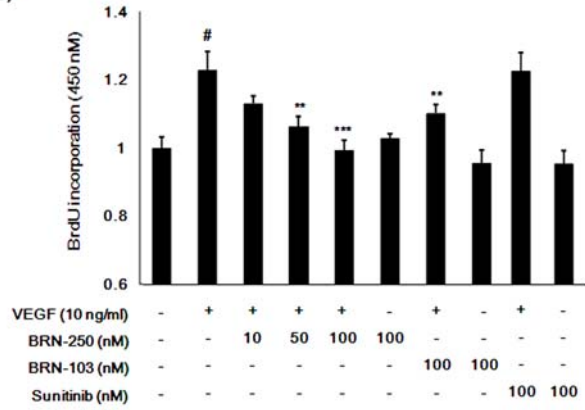
25. Ferrara, N.; Gerber, H. P.; LeCouter, J. *Nat. Med.* **2003**, *9*, 669.
26. Olsson, A. K.; Dimberg, A.; Kreuger, J.; Claesson-Welsh, L. *Nat. Rev. Mol. Cell Biol.* **2006**, *7*, 359.
27. Cantley, L. C. *Science* **2002**, *296*, 1655.
28. Wymann, M. P.; Pirola, L. *Biochim. Biophys. Acta.* **1998**, *1436*, 127.
29. Chavakis, E.; Dernbach, E.; Hermann, C.; Mondorf, U. F.; Zeiher, A. M.; Dimmeler, S. *Circulation* **2001**, *103*, 2102.
30. Morales-Ruiz, M.; Fulton, D.; Sowa, G.; Languino, L. R.; Fujio, Y.; Walsh, K.; Sessa, W. C. *Circ. Res.* **2000**, *86*, 892.
31. Yang, L.; Dan, H. C.; Sun, M.; Liu, Q.; Sun, X. M.; Feldman, R. I.; Hamilton, A. D.; Polokoff, M.; Nicosia, S. V.; Herlyn, M.; Sebt, S. M.; Cheng, J. Q. *Cancer Res.* **2004**, *64*, 4394.
32. MVD **2010.4.2** for Windows in MolegroApS
33. Hasegawa, M.; Nishigaki, N.; Washio, Y.; Kano, K.; Harris, P. A.; Sato, H.; Mori, I.; West, R. I.; Shibahara, M.; Toyoda, H.; Wang, L.; Nolte, R. T.; Veal, J. M.; Cheung, M. *J. Med. Chem.* **2007**, *50*, 4453.

Fig 1

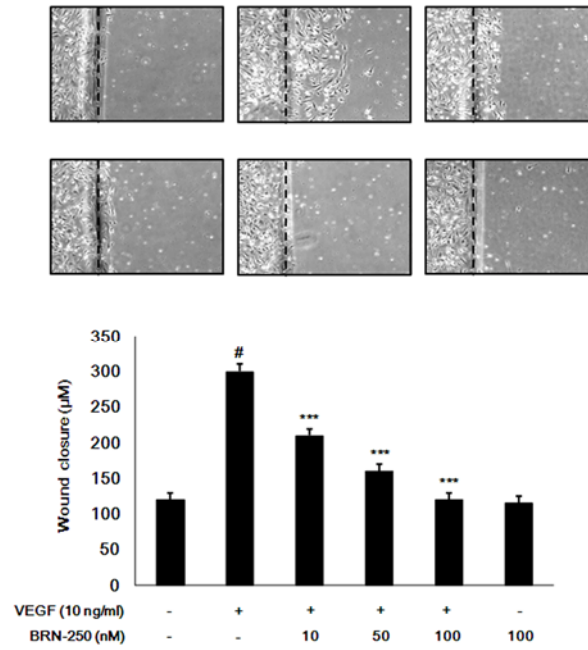
(A)



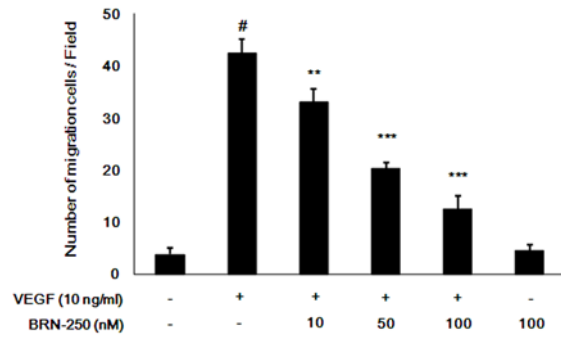
(B)



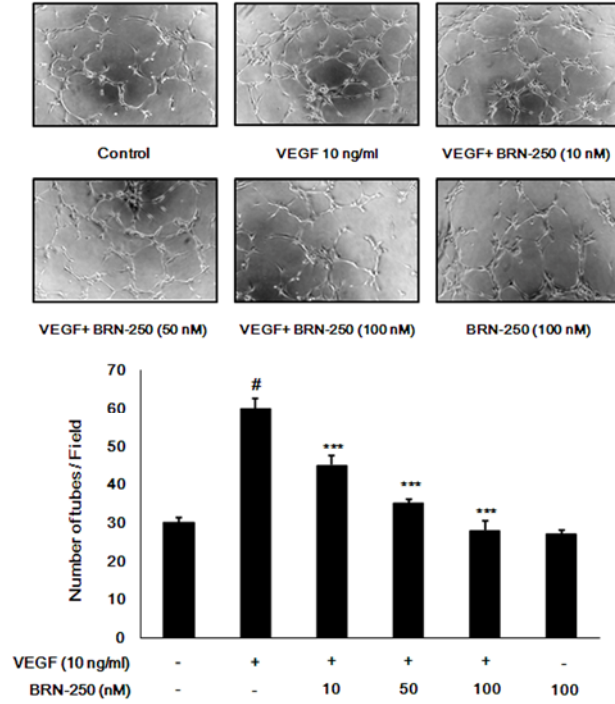
(A)



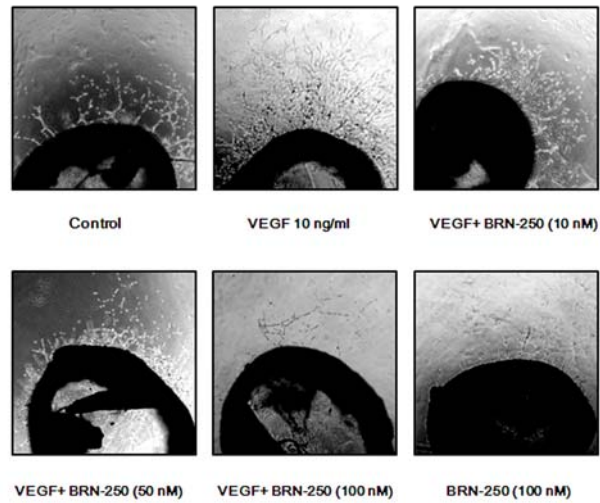
(B)



(A)

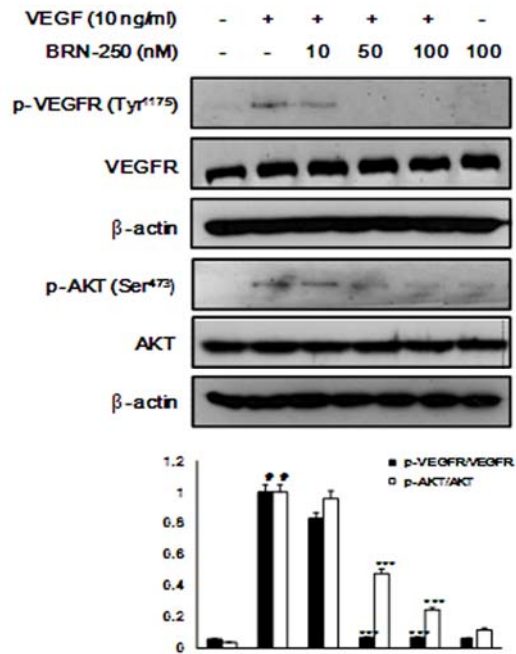


(B)



A

(A)



(B)

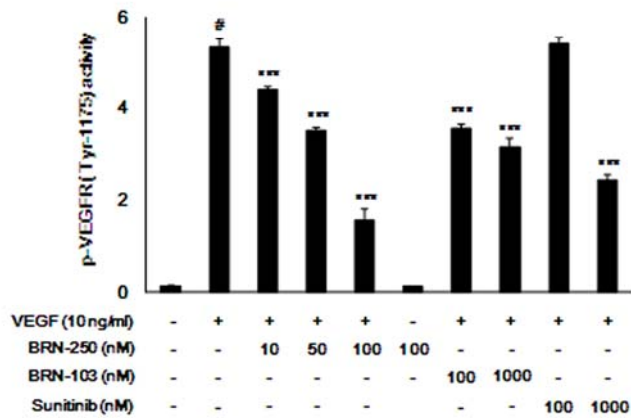
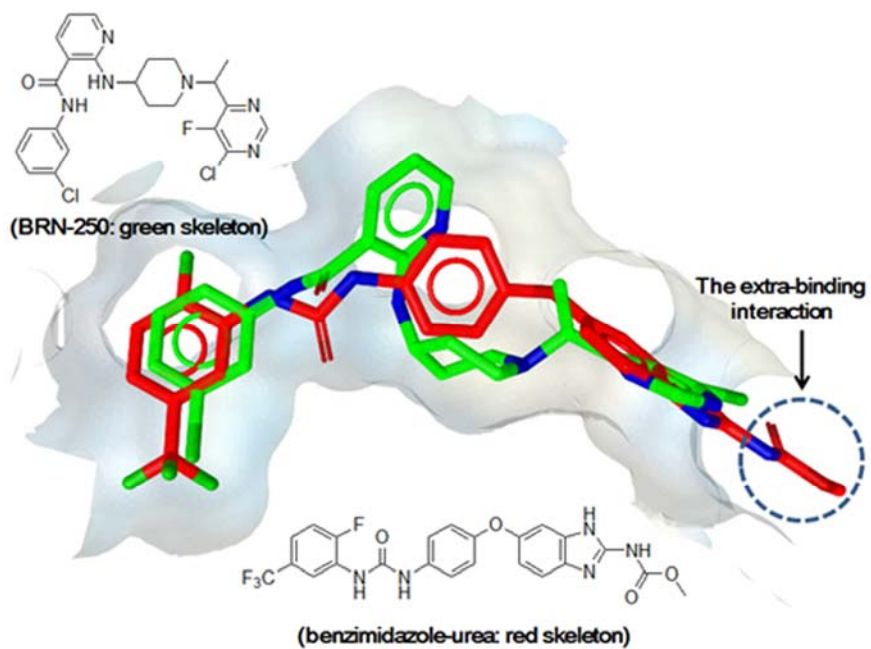
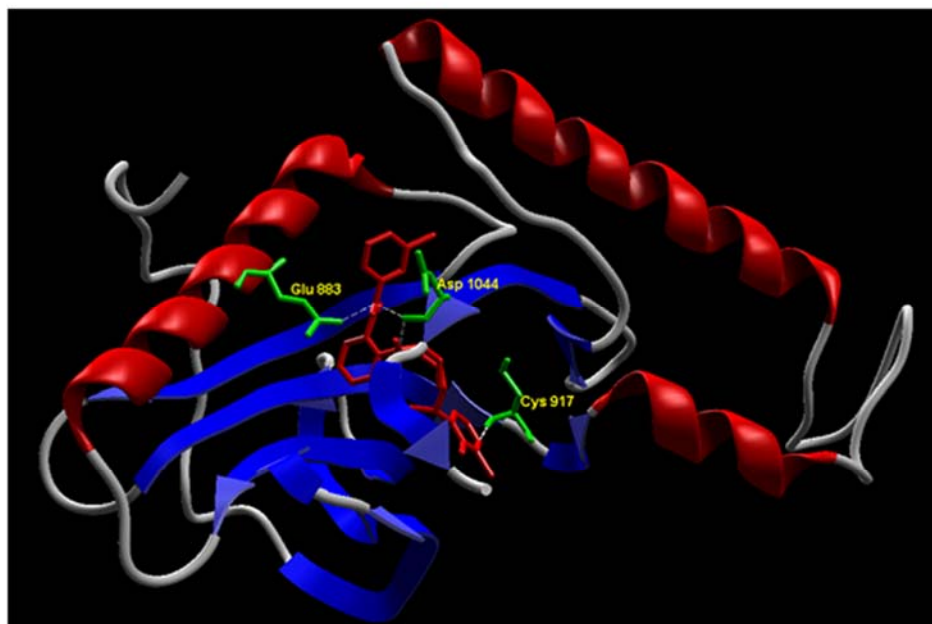


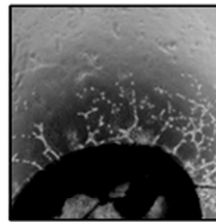
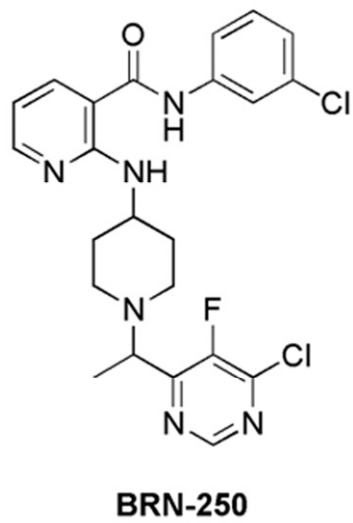
Fig 5

(A)

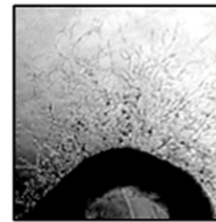


(B)

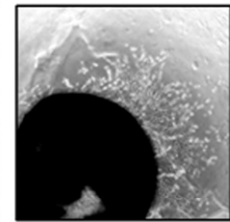




Control



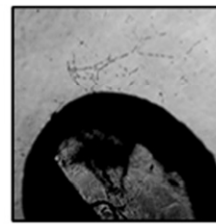
VEGF 10 ng/ml



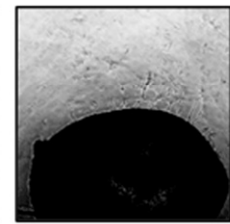
VEGF+BRN-250 (10 nM)



VEGF+BRN-250 (50 nM)



VEGF+BRN-250 (100 nM)



BRN-250 (100 nM)

ACCEPTED MANUSCRIPT